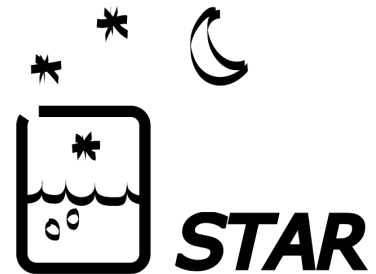


# Measurement of $^{16}\text{O}(\gamma,\alpha)^{12}\text{C}$ with a bubble chamber and a bremsstrahlung beam



Superheated Target for Astrophysics  
Research (STAR)



Claudio Ugalde, for the STAR  
collaboration.

Argonne, UChicago, JLab, Fermilab



B. DiGiovine  
D. Henderson  
R. J. Holt  
K. E. Rehm



THE UNIVERSITY OF  
**CHICAGO**

C. Ugalde  
A. Robinson

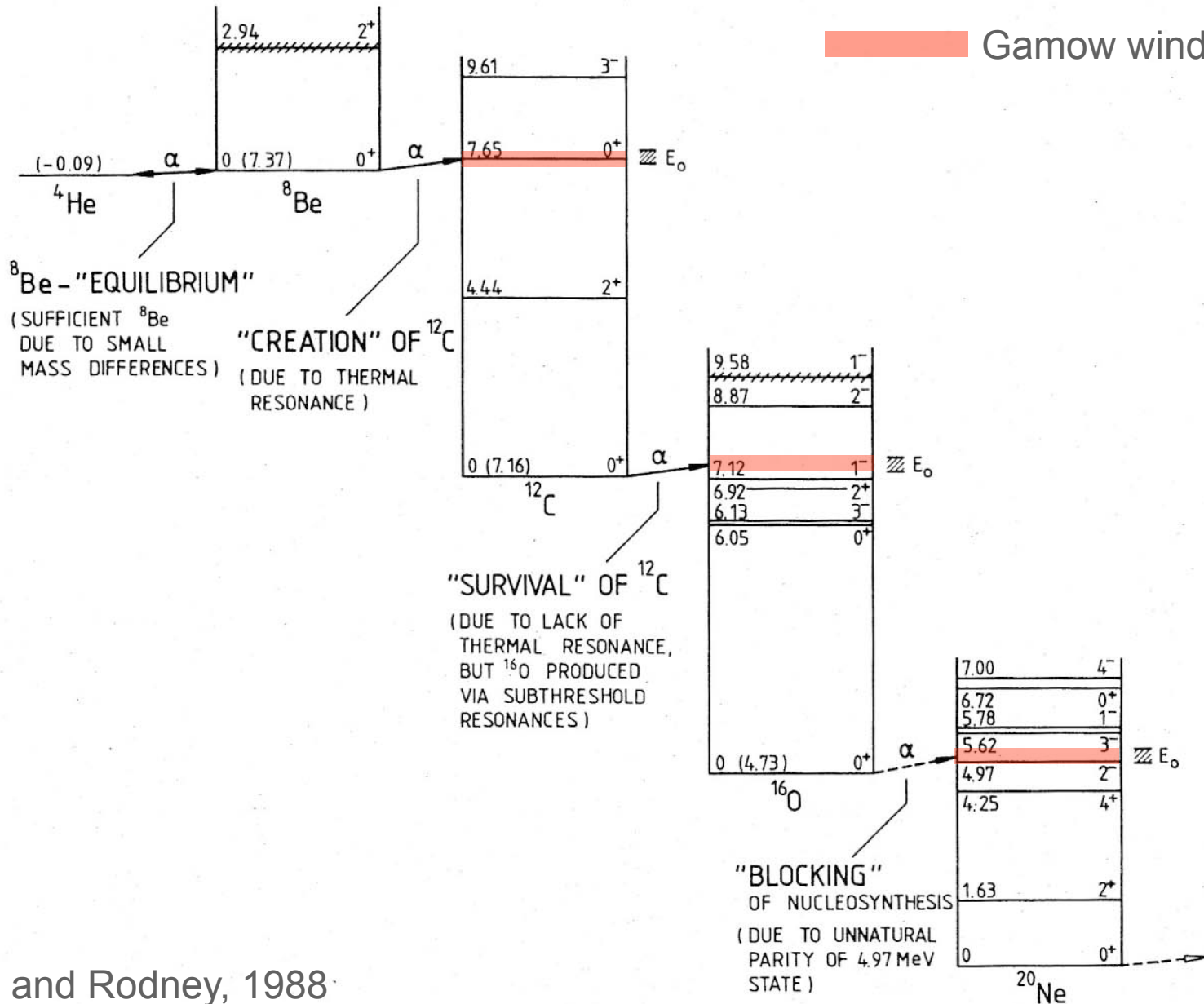


A. Sonnenschein



R. Suleiman  
A. Freyberger  
J. Grames  
R. Kazimi  
M. Poelker  
R. Mammei  
D. Meekins  
Y. Roblin  
V. Vylet,  
G. Kharashvili  
P. Degtiarenko

 Gamow window

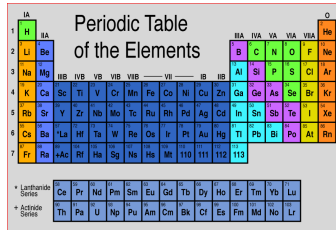


Rolfs and Rodney, 1988



# $^{12}\text{C}(\alpha,\gamma)^{16}\text{O}$ Reaction

Key reaction for nucleosynthesis in massive stars, progenitors of Type Ia Supernovae, White Dwarf ages.



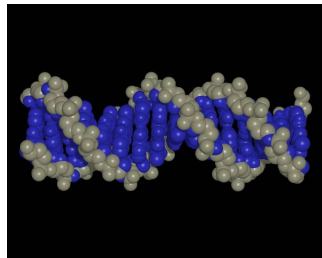
Periodic Table of the Elements

The image shows a standard periodic table of elements, color-coded by groups. It includes the main groups (IA to VIIA), transition metals (IB to VIIIB), and the lanthanide and actinide series at the bottom.

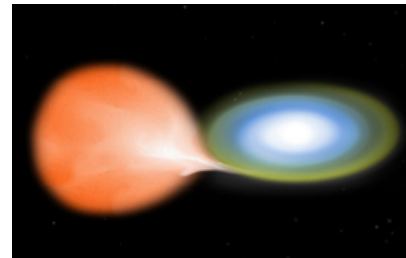
Affects the synthesis of most of the elements of the periodic table



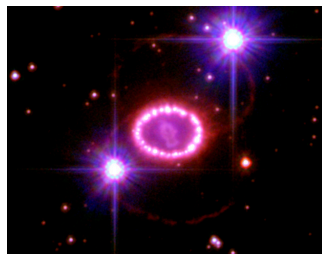
Determines whether for a given initial mass, a star will become a black hole or a neutron star



Sets the C to O ratio in the universe



The variation of the C/O ratio in the progenitor might be a cause of the variation of SNIa brightness

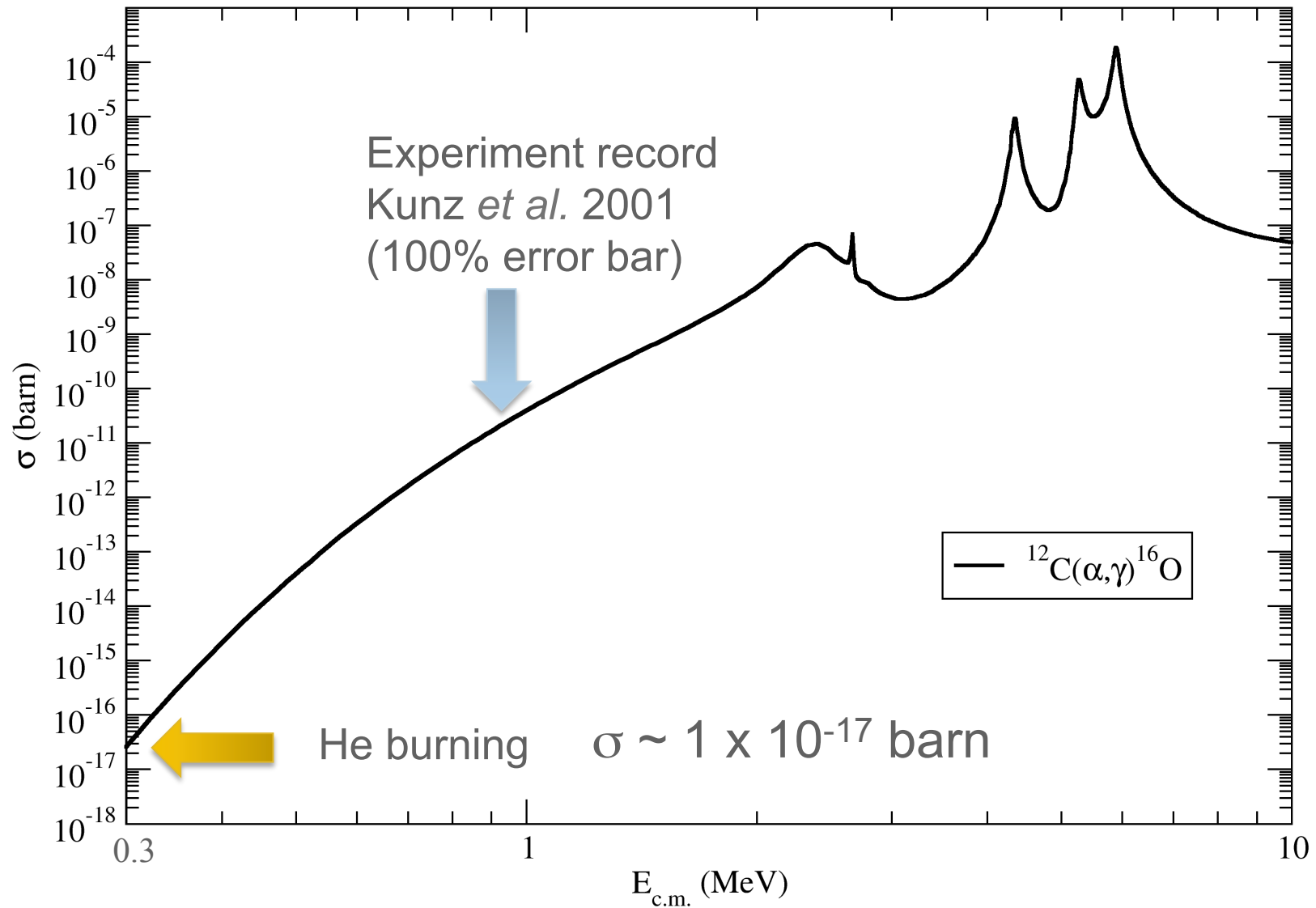


Determines the minimum mass a star requires to become a core collapse supernova



Affects the constraints on the age of stellar populations from White Dwarfs





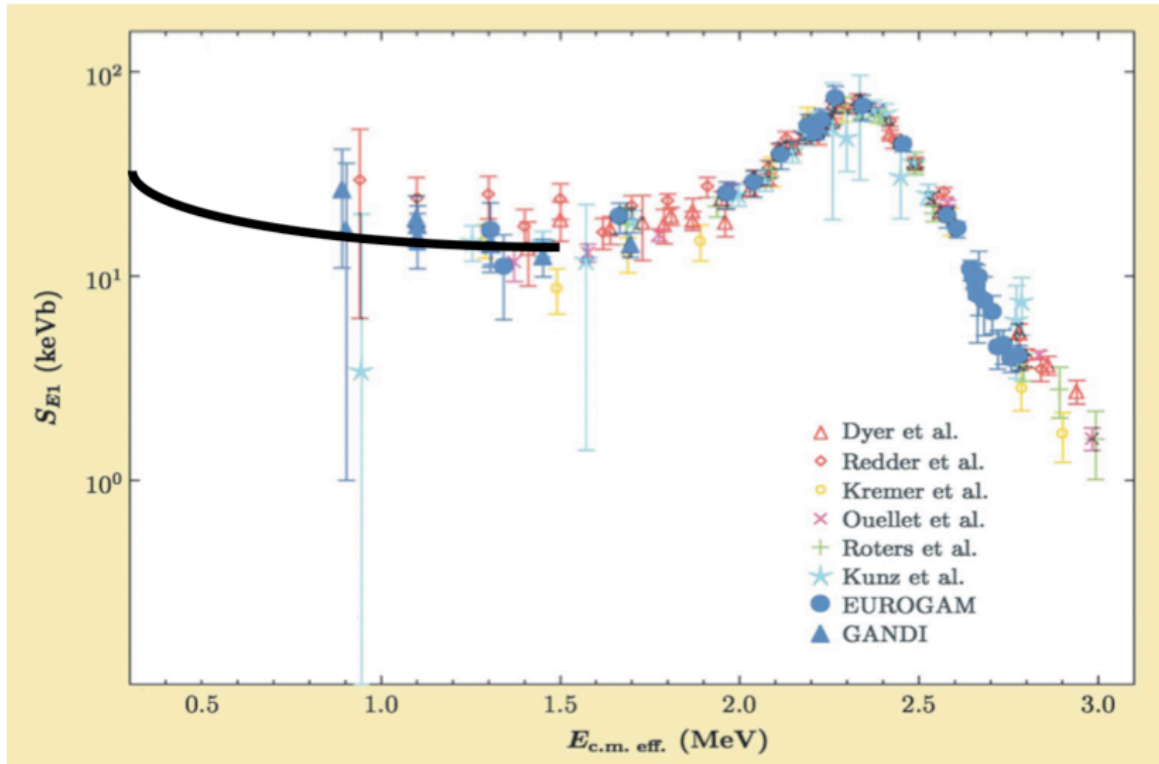
$$N_A \langle \sigma v \rangle = N_A \sqrt{\frac{8}{\pi \mu (kT)^3}} \int_0^\infty \sigma(E) E \exp\left(-\frac{E}{kT}\right) dE$$



# Astrophysical S-factor for $^{12}\text{C}(\alpha,\gamma)^{16}\text{O}$

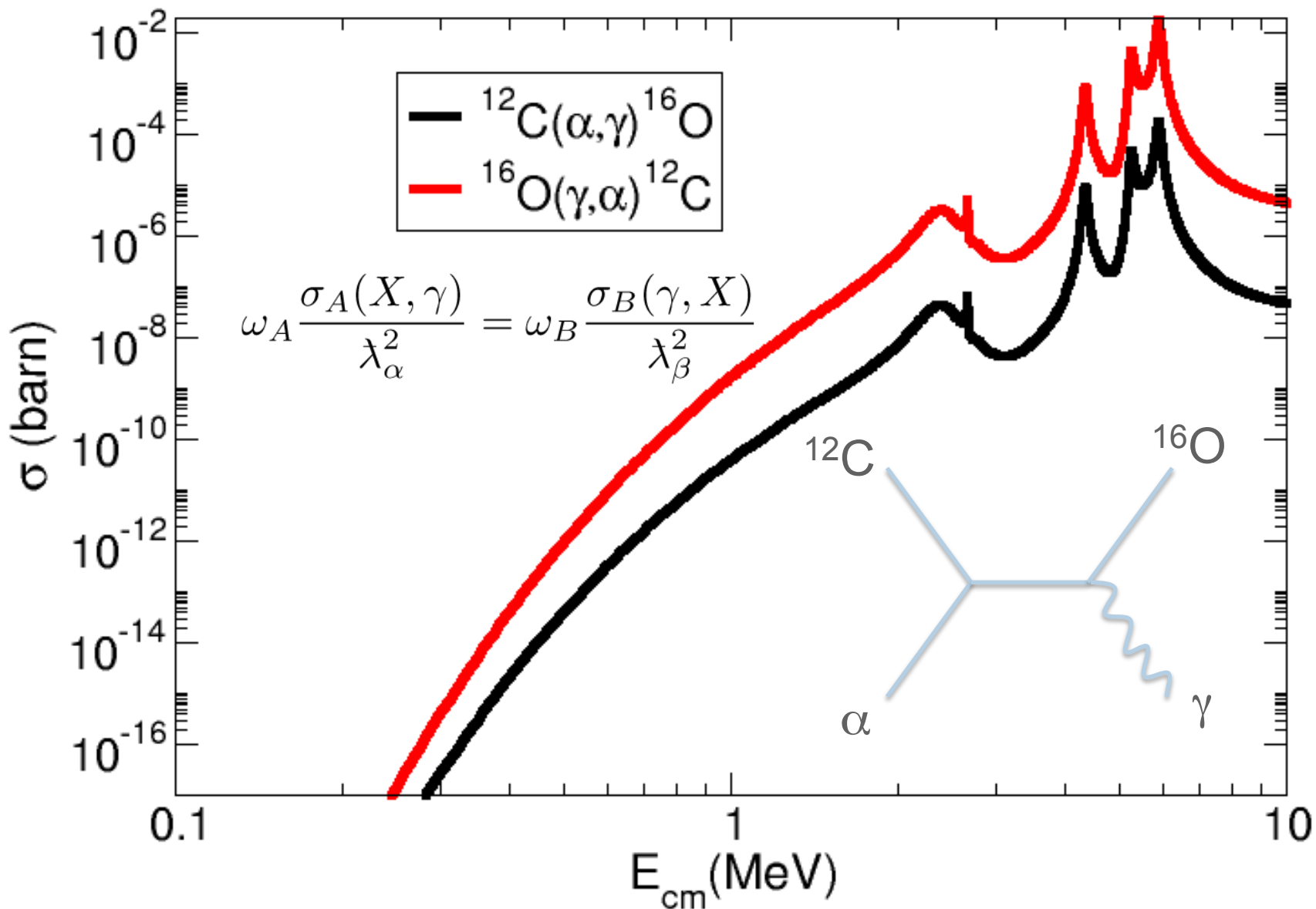
Stellar helium burning at  $E=300\text{ keV}$

$$S = E \sigma \exp(2\pi\eta)$$

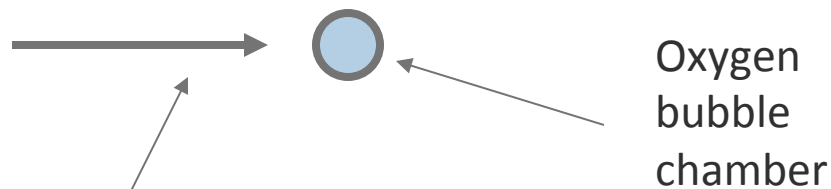
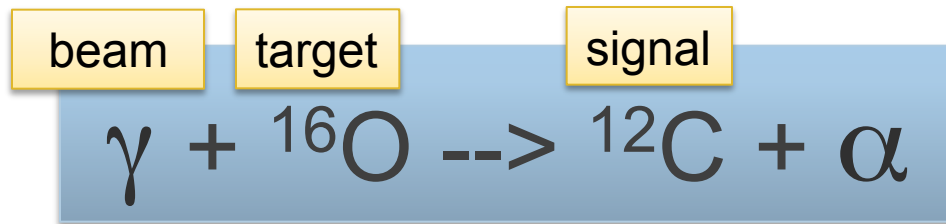


Author	S(300keV) (keV-b)
Buchmann (2005)	102-198
Caughlan and Fowler (1988)	120-220
Hammer (2005)	162+-39

Time reversal symmetry: x100 gain in cross section



# New approach: Inverse reaction + Bubble chamber + Bremsstrahlung



Monochromatic  $\gamma$  beam from HI $\gamma$ S  
 $\sim 10^{7-8}$   $\gamma/s$

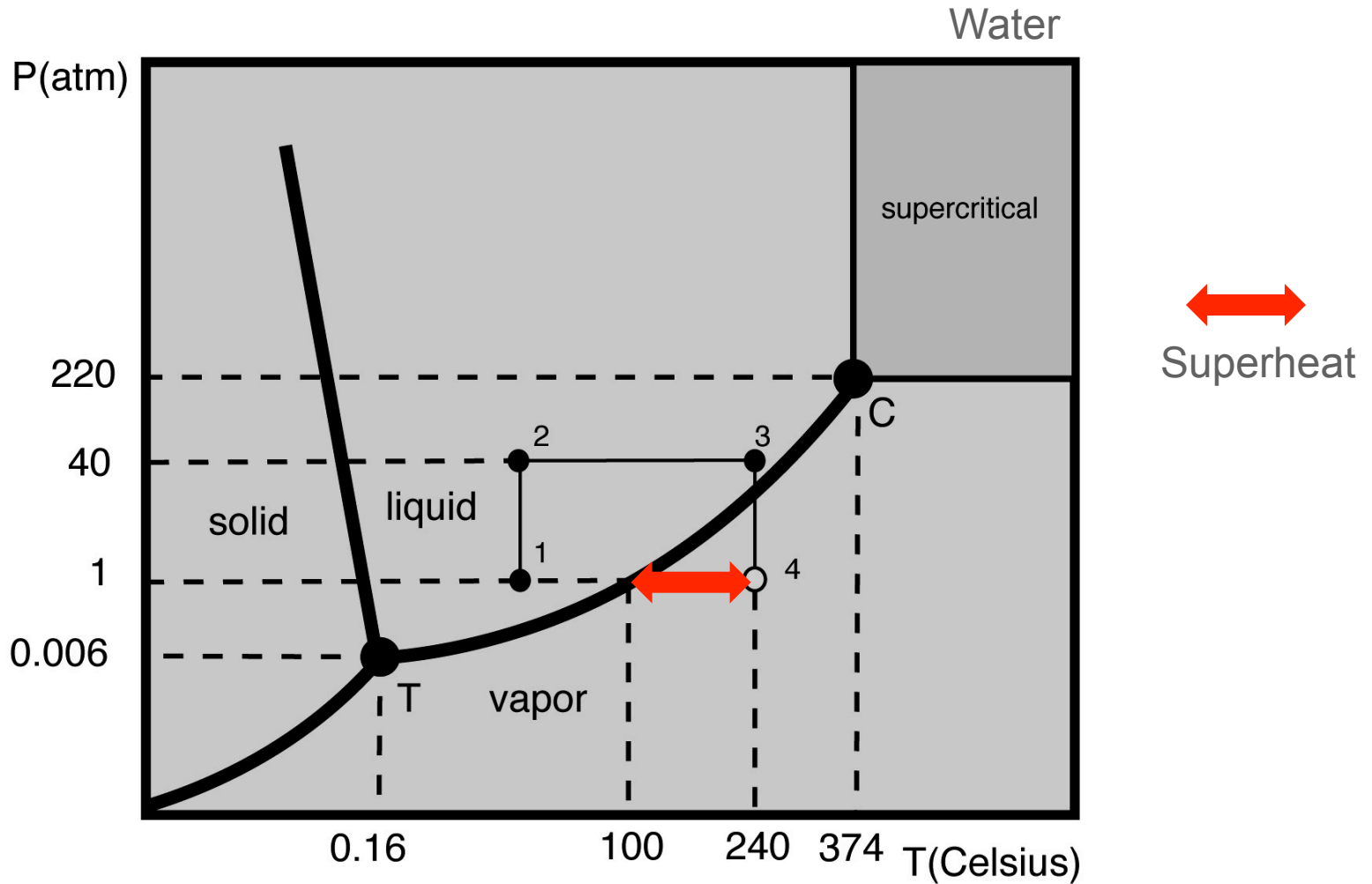
Bremsstrahlung from JLab  $\sim 4 \times 10^9$   $\gamma/s$  (top 250 keV)

- Extra gain (x100) by measuring time inverse reaction
- Target density up to  $\times 10^6$  higher than conventional targets.
- Superheated water will nucleate from  $\alpha$  and  ${}^{12}\text{C}$  recoils
- Electromagnetic debris (degraded electrons and gammas, or positrons) that escape the collimator/electron beam do NOT trigger nucleation (The detector is insensitive to  $\gamma$ -rays by at least 1 part in  $10^{11}$ ).
- Tested at HI $\gamma$ S

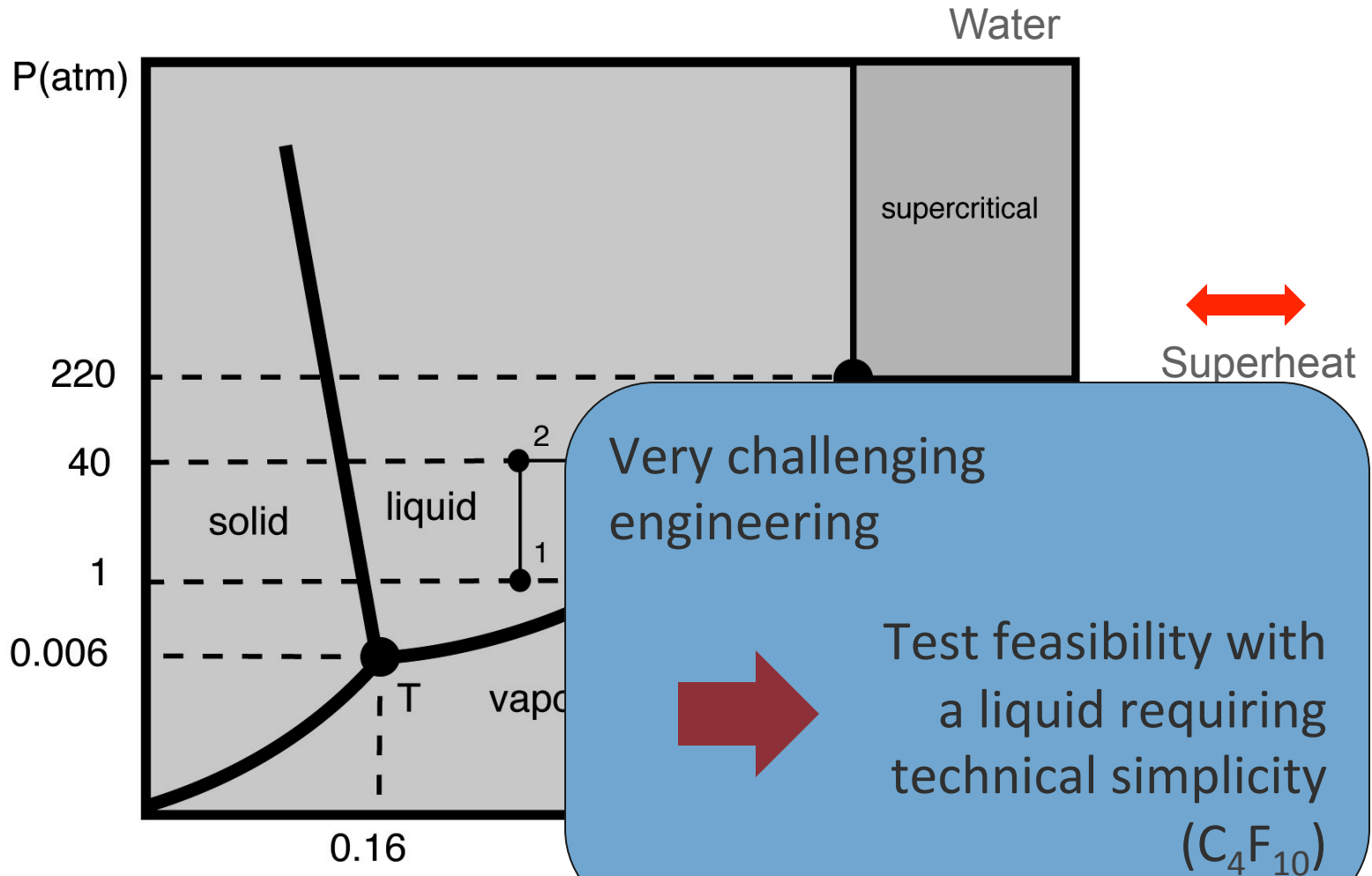




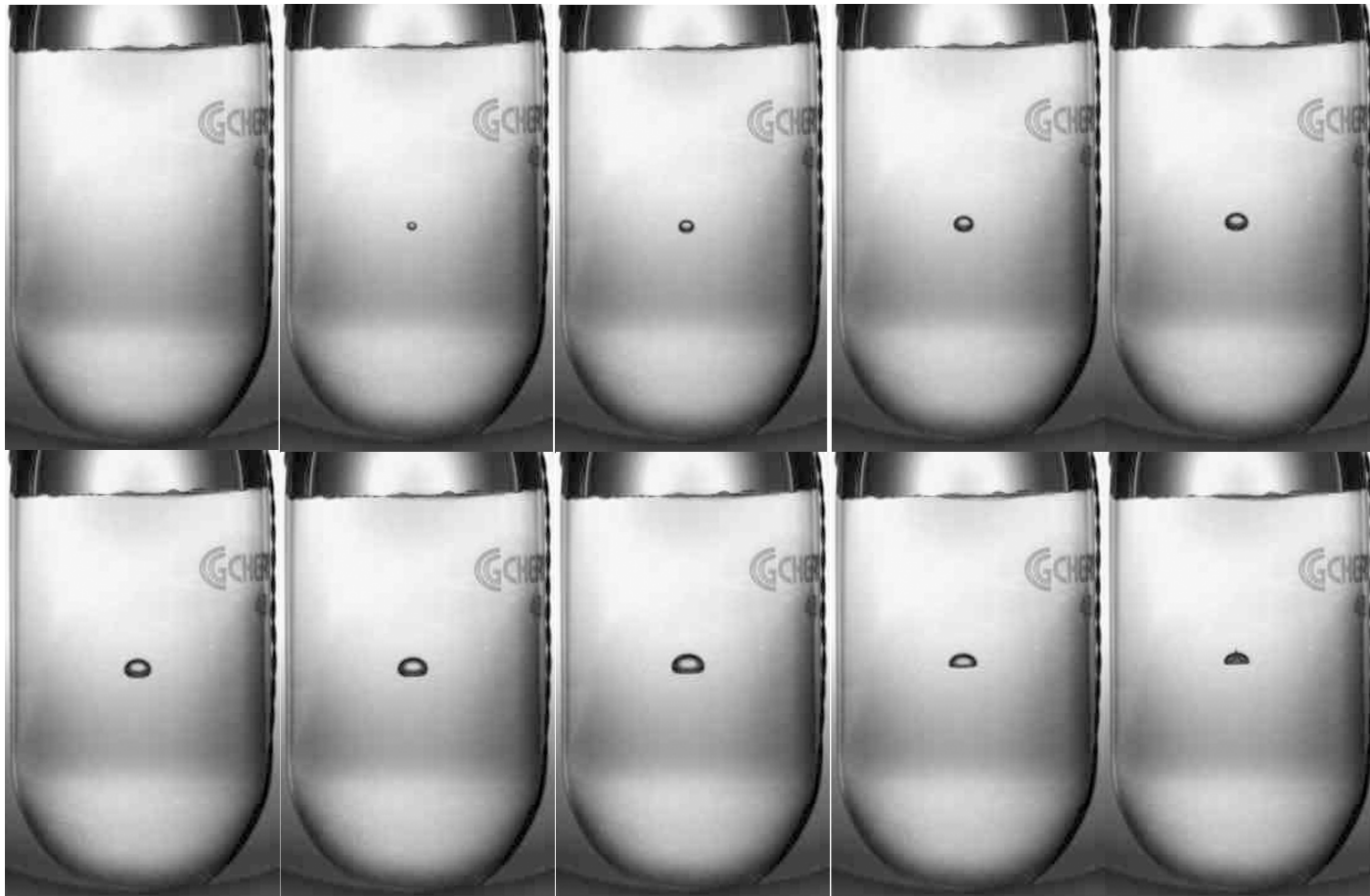
# Superheating of liquids



# Superheating of liquids

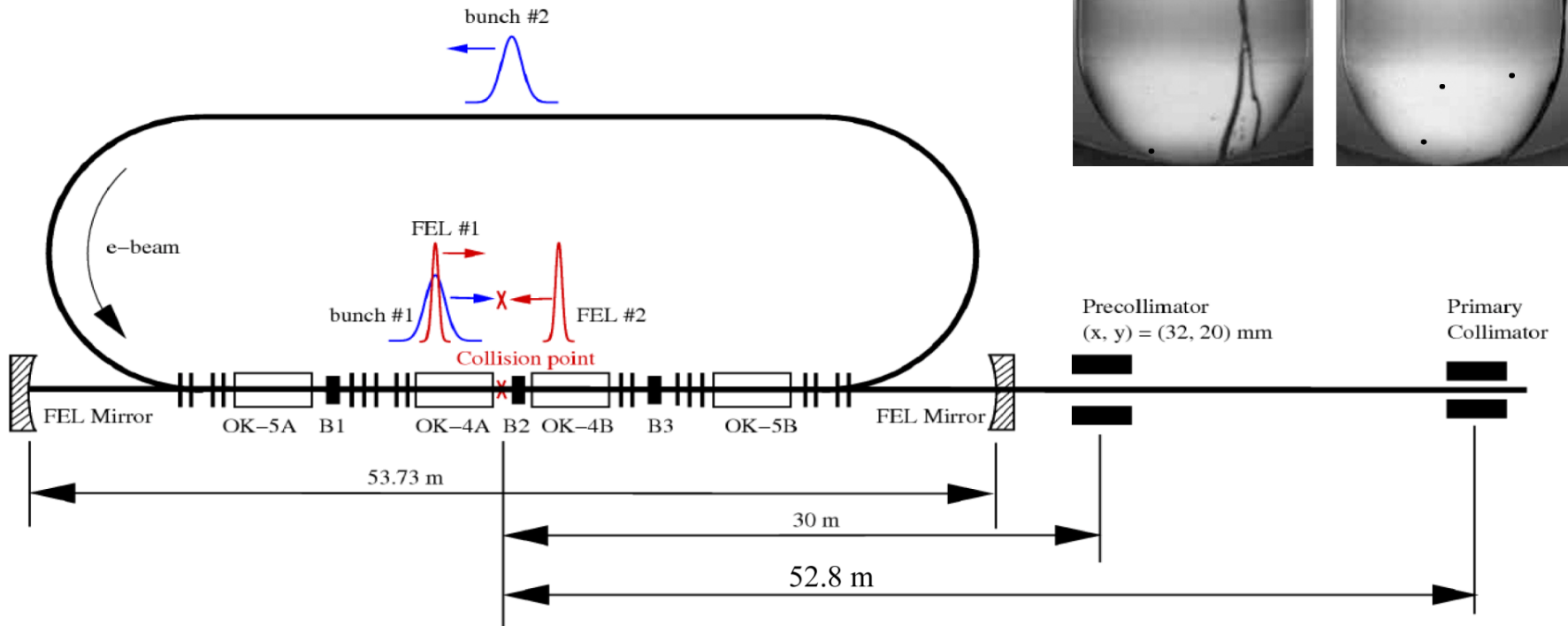


# Bubble growth and quenching. $^{19}\text{F}(\gamma, \alpha)^{15}\text{N}$ in R134a

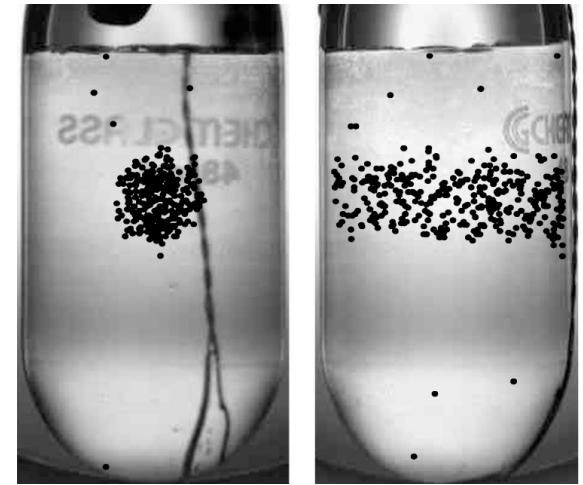
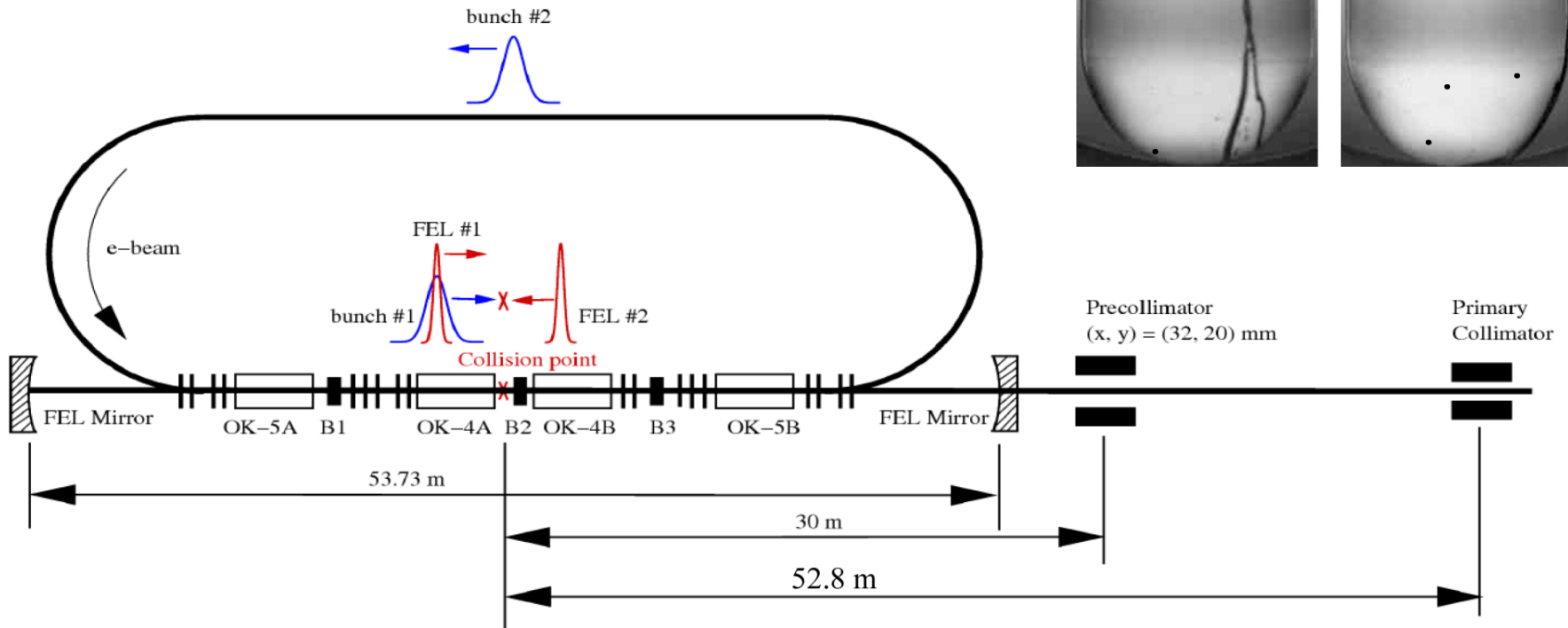


$\Delta t = 10 \text{ ms}$

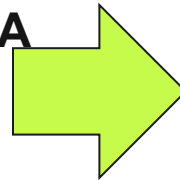
# H $\gamma$ S Photon Beam



# H $\gamma$ S Photon Beam



**E (electron) ~ 500 MeV,  $I_e=50\text{mA}$**   
**+**  
 **$2 \times 10^{-10}$  torr vacuum**



**Strong bremsstrahlung  
background component**



Contents lists available at SciVerse ScienceDirect

Physics Letters B

www.elsevier.com/locate/physletb



## First determination of an astrophysical cross section with a bubble chamber: The $^{15}\text{N}(\alpha, \gamma)^{19}\text{F}$ reaction

C. Ugalde<sup>a,\*</sup>, B. DiGiovine<sup>b</sup>, D. Henderson<sup>b</sup>, R.J. Holt<sup>b</sup>, K.E. Rehm<sup>b</sup>, A. Sonnenschein<sup>c</sup>, A. Robinson<sup>d</sup>,  
R. Raut<sup>e,f,1</sup>, G. Rusev<sup>e,f,2</sup>, A.P. Tonchev<sup>e,f,3</sup>

<sup>a</sup> Department of Astronomy and Astrophysics, University of Chicago, Chicago, IL 60637, USA

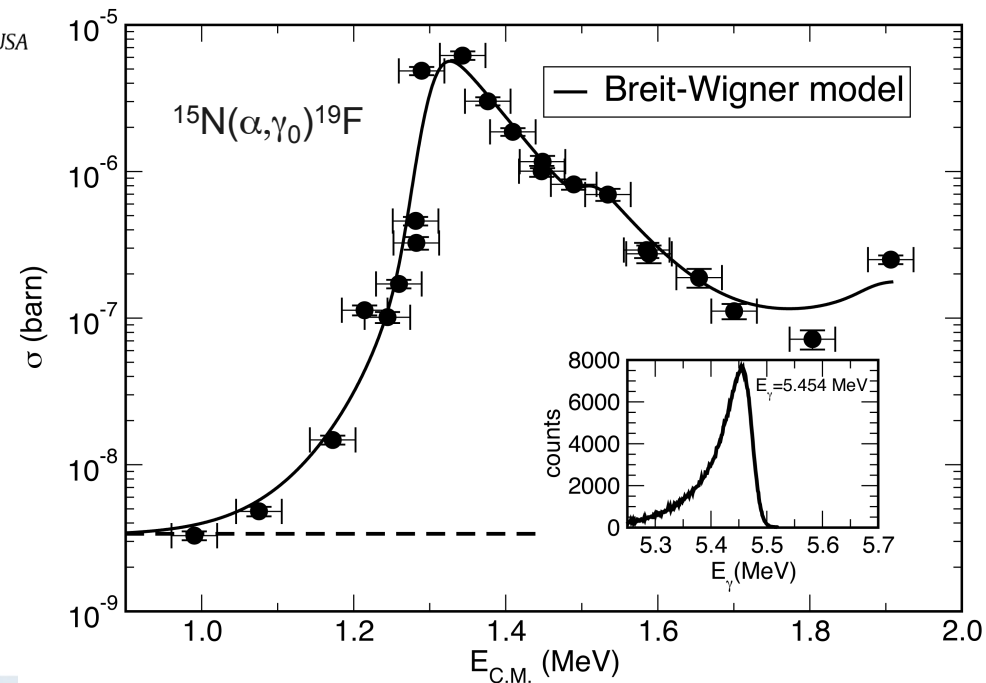
<sup>b</sup> Physics Division, Argonne National Laboratory, Argonne, IL 60439, USA

<sup>c</sup> Fermi National Accelerator Laboratory, Batavia, IL 60510, USA

<sup>d</sup> Department of Physics, University of Chicago, Chicago, IL 60637, USA

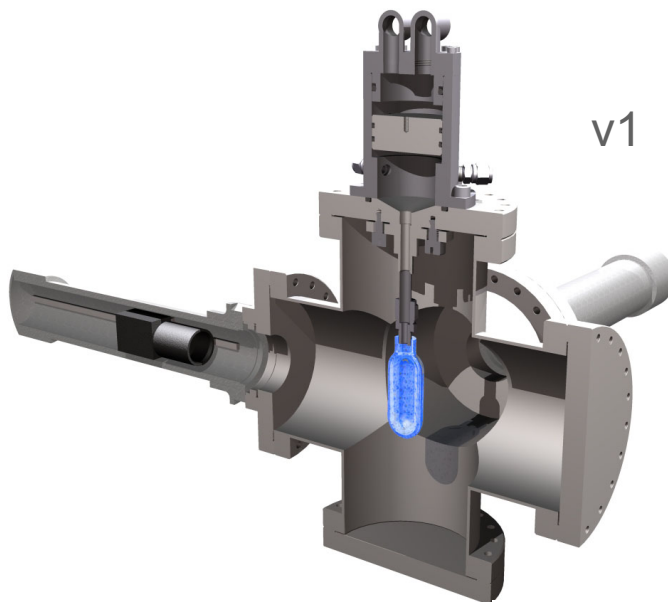
<sup>e</sup> Department of Physics, Duke University, Durham, NC 27708, USA

<sup>f</sup> Triangle Universities Nuclear Laboratory, Durham, NC 27708, USA

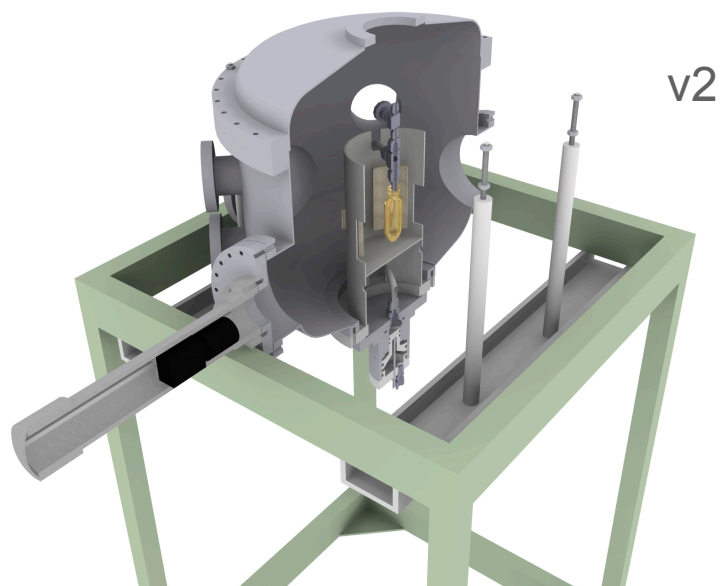
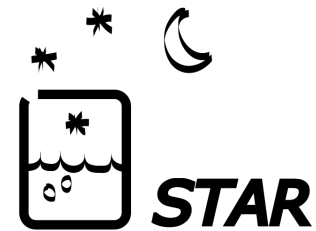


## Liquids tested

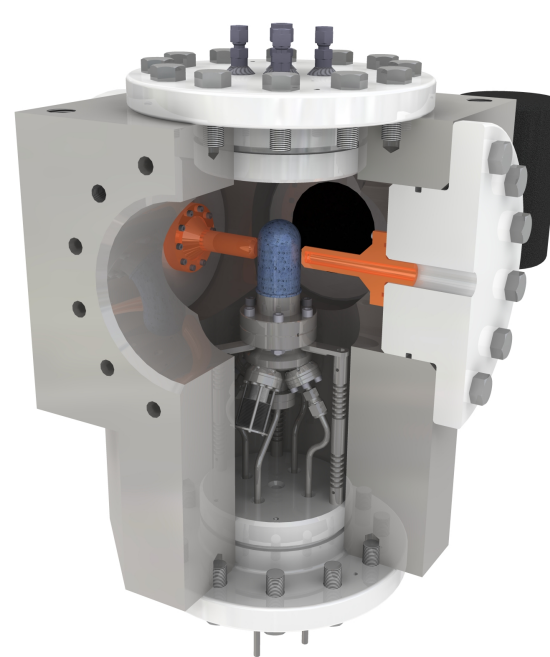
- $\text{CH}_2\text{FCF}_3$
- $\text{C}_4\text{F}_{10}$
- $\text{H}_2\text{O}$
- $\text{N}_2\text{O}$
- $\text{CO}_2$



v1



v2



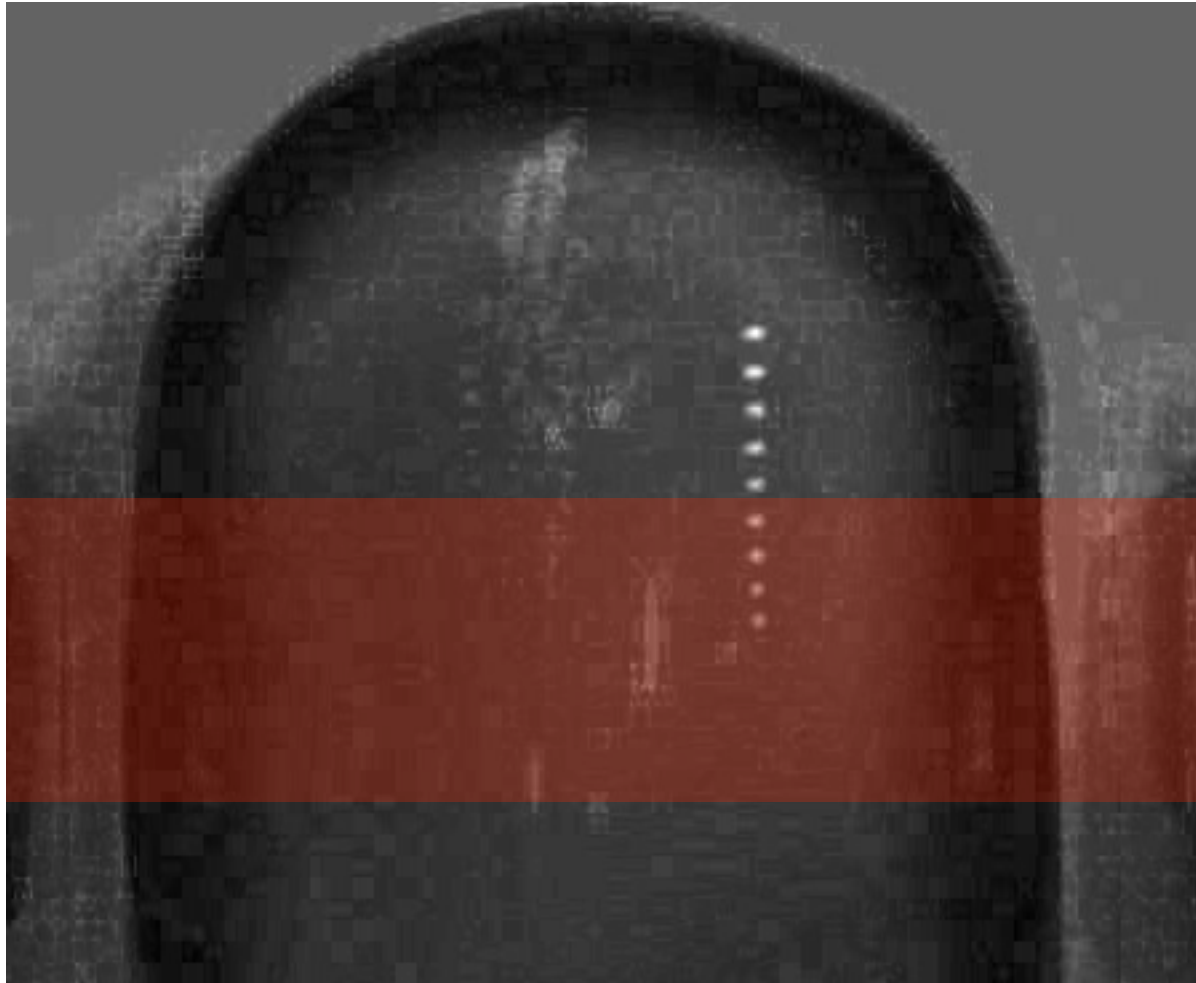
v3



$N_2O$

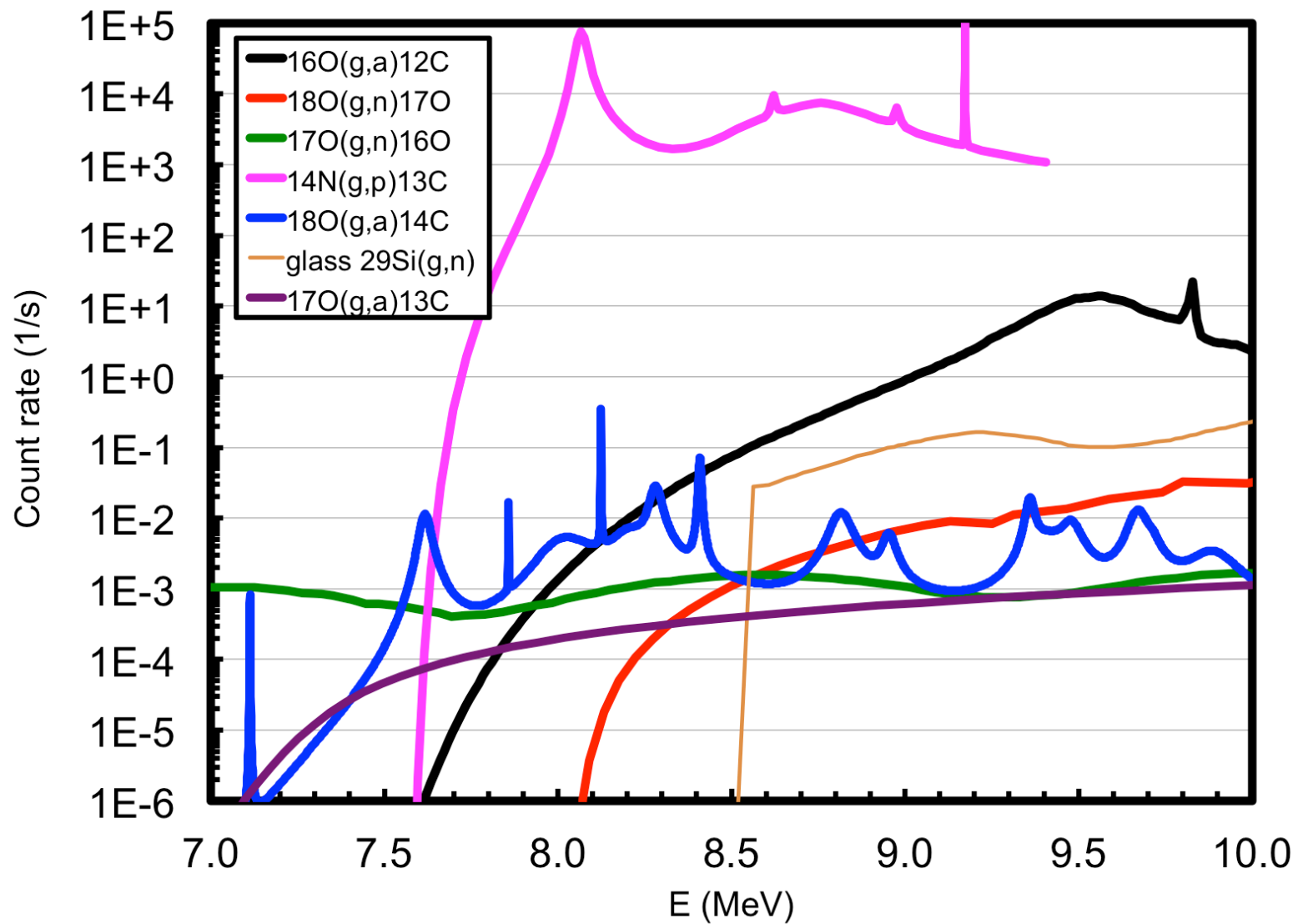
First  $\gamma$  + oxygen  $\rightarrow$  alpha + carbon bubble

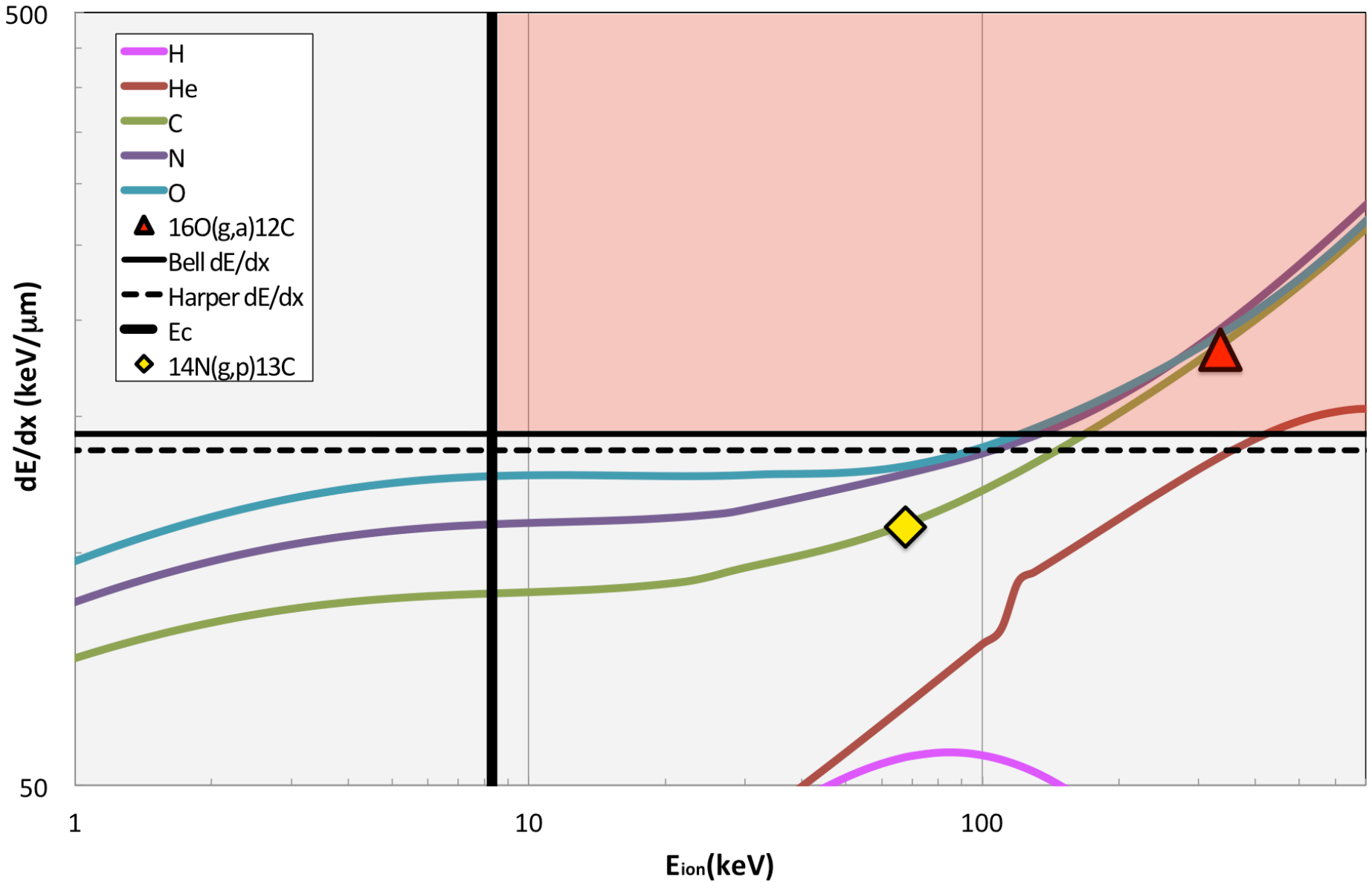
April 2013



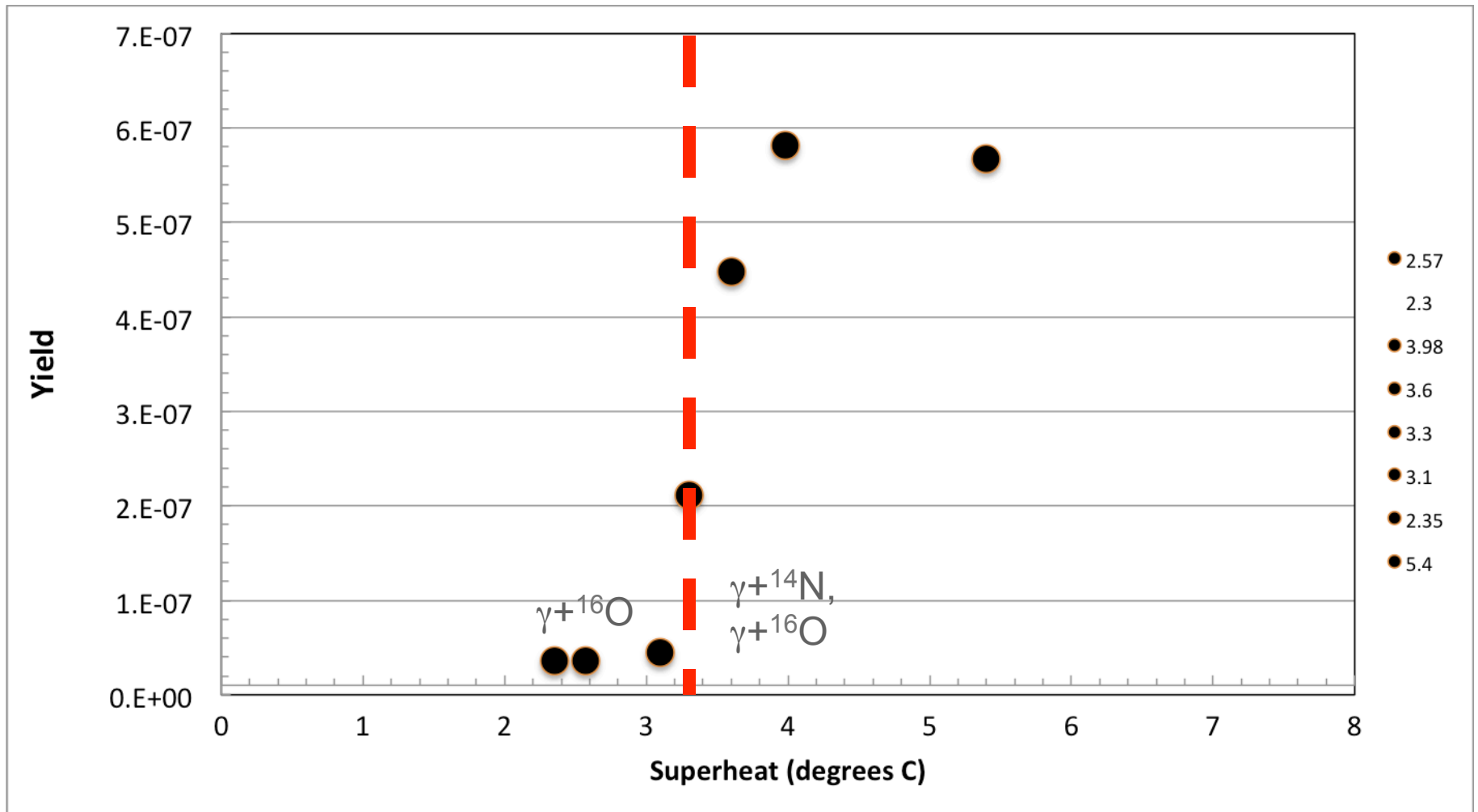


$\text{N}_2\text{O}$  count rate contributions,  $I_\gamma = 1 \times 10^8 \text{ } \gamma/\text{s}$   
L = 3.6 cm, x1000 depleted liquid





# N<sub>2</sub>O efficiency curve, HI $\gamma$ S April 2013. E $\gamma$ = 9.7MeV



# Bremsstrahlung beams at JLab injector

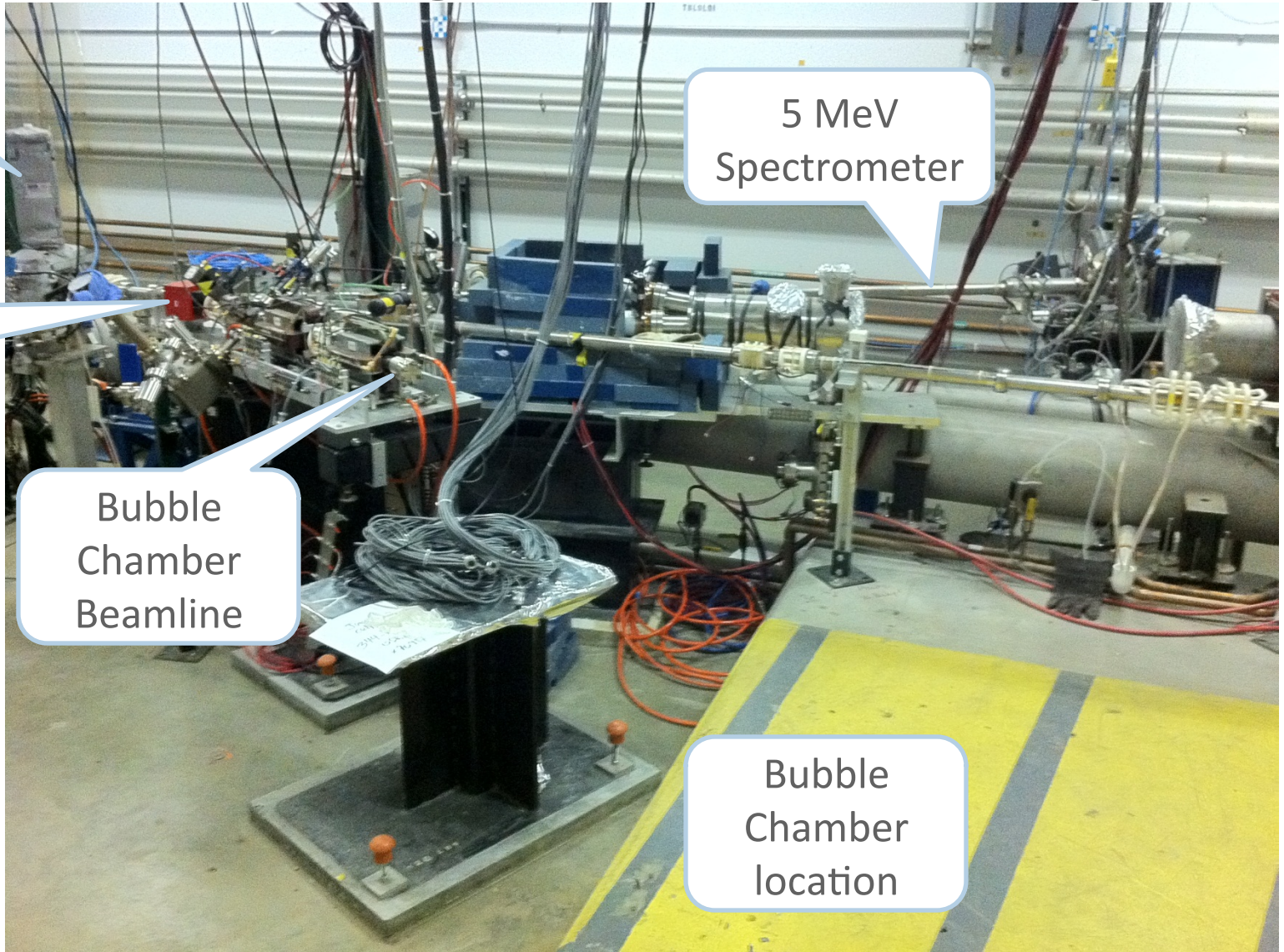
BCM

5 MeV  
Dipole

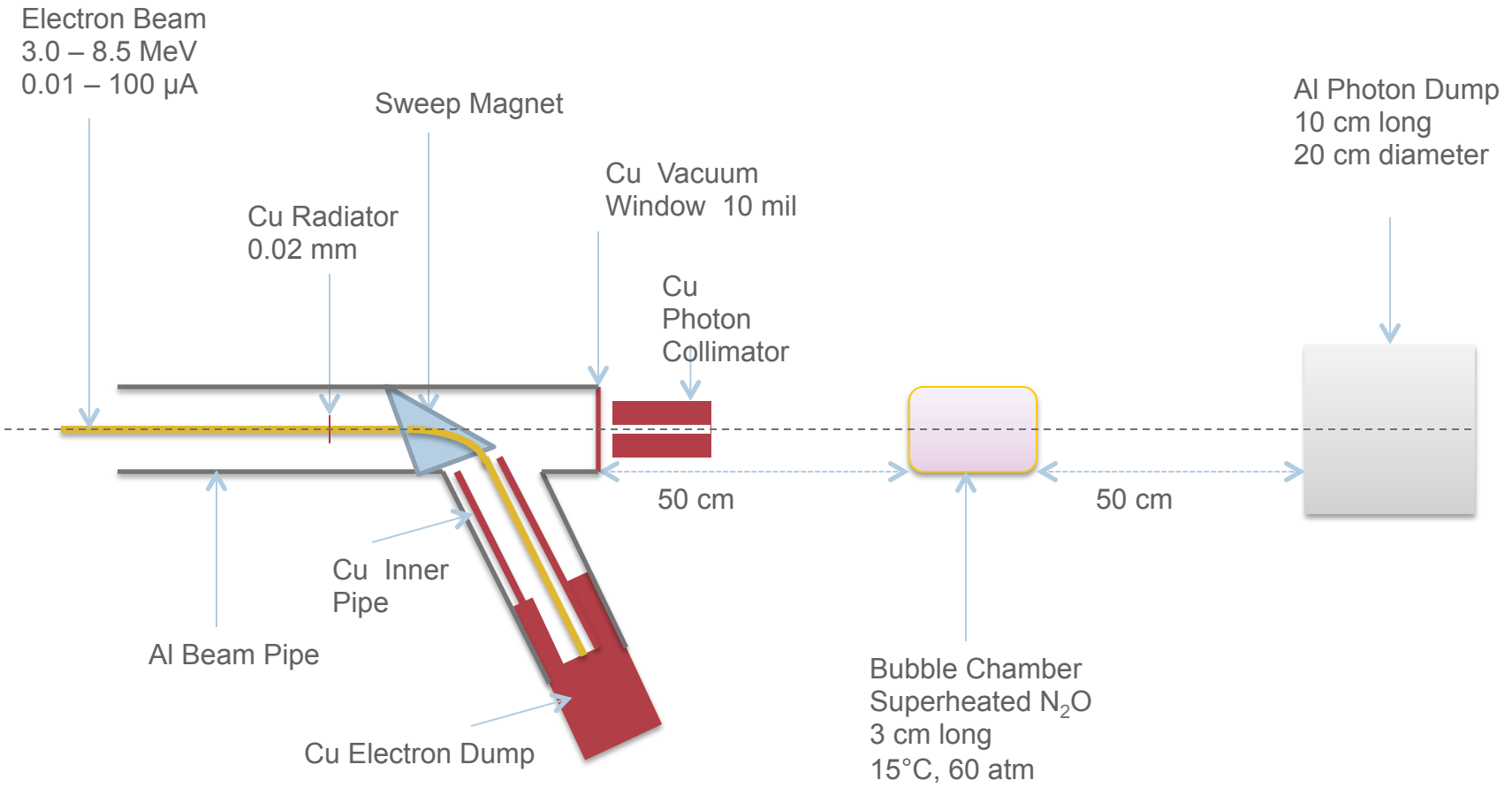
Bubble  
Chamber  
Beamline

5 MeV  
Spectrometer

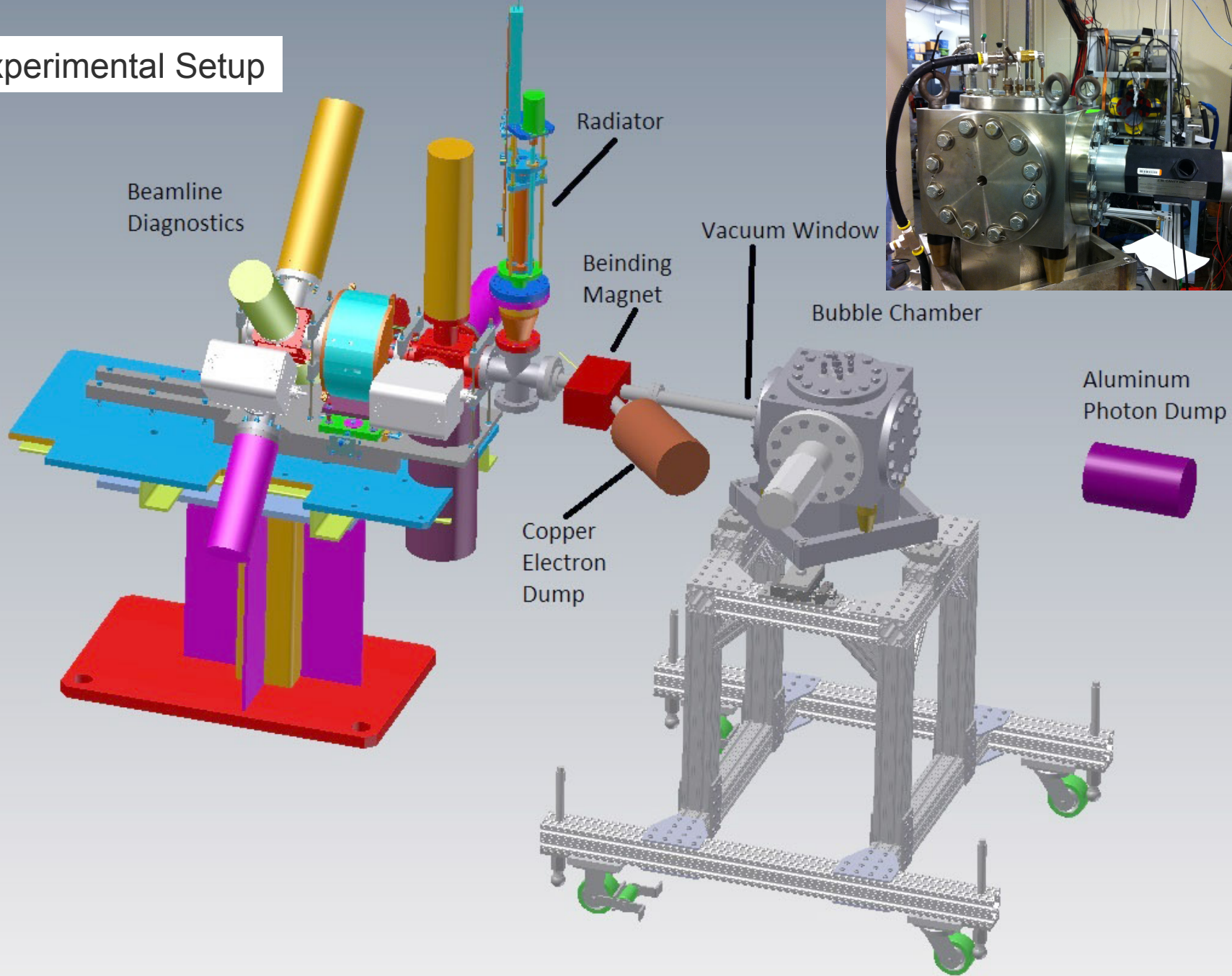
Bubble  
Chamber  
location

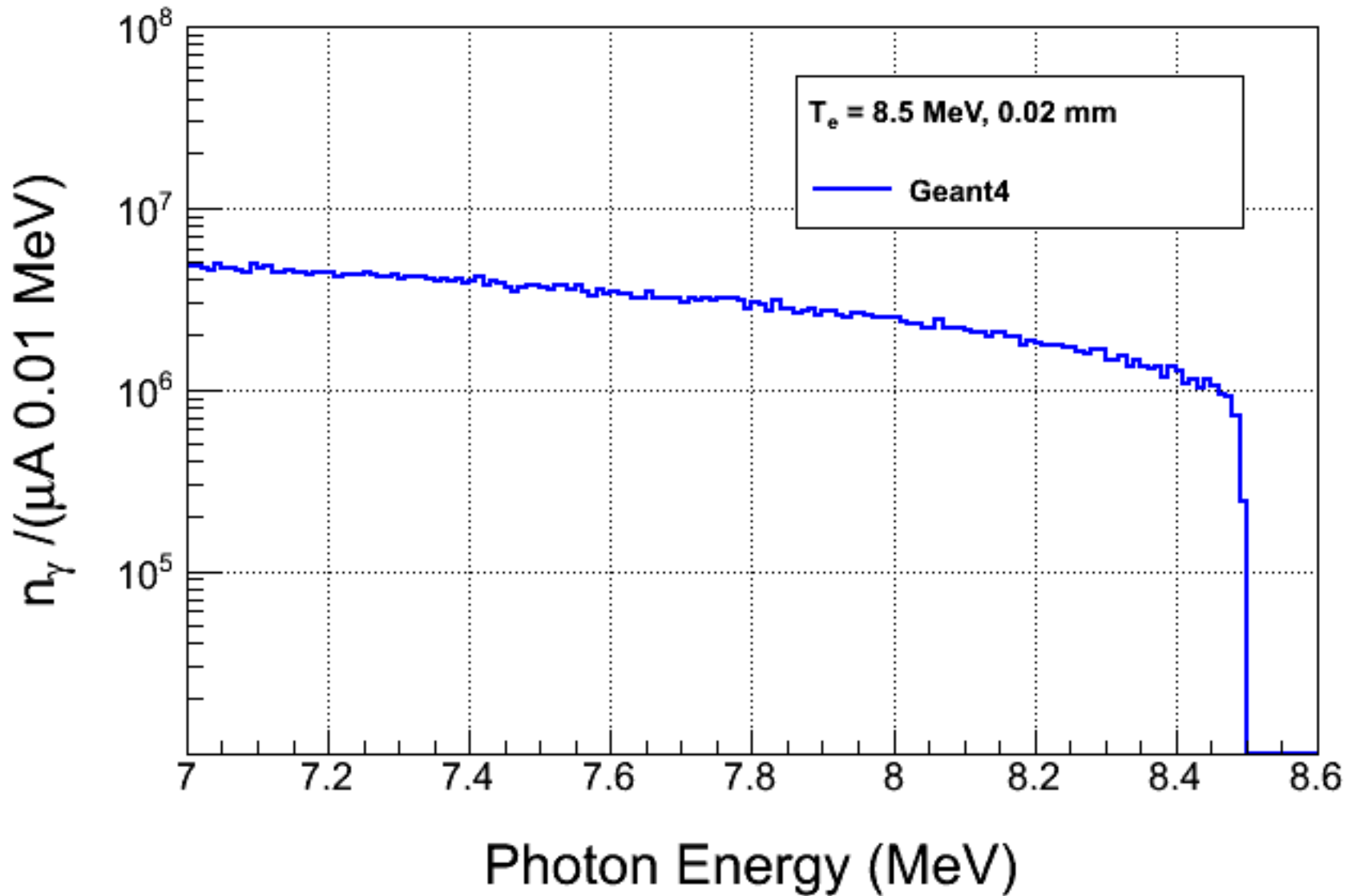


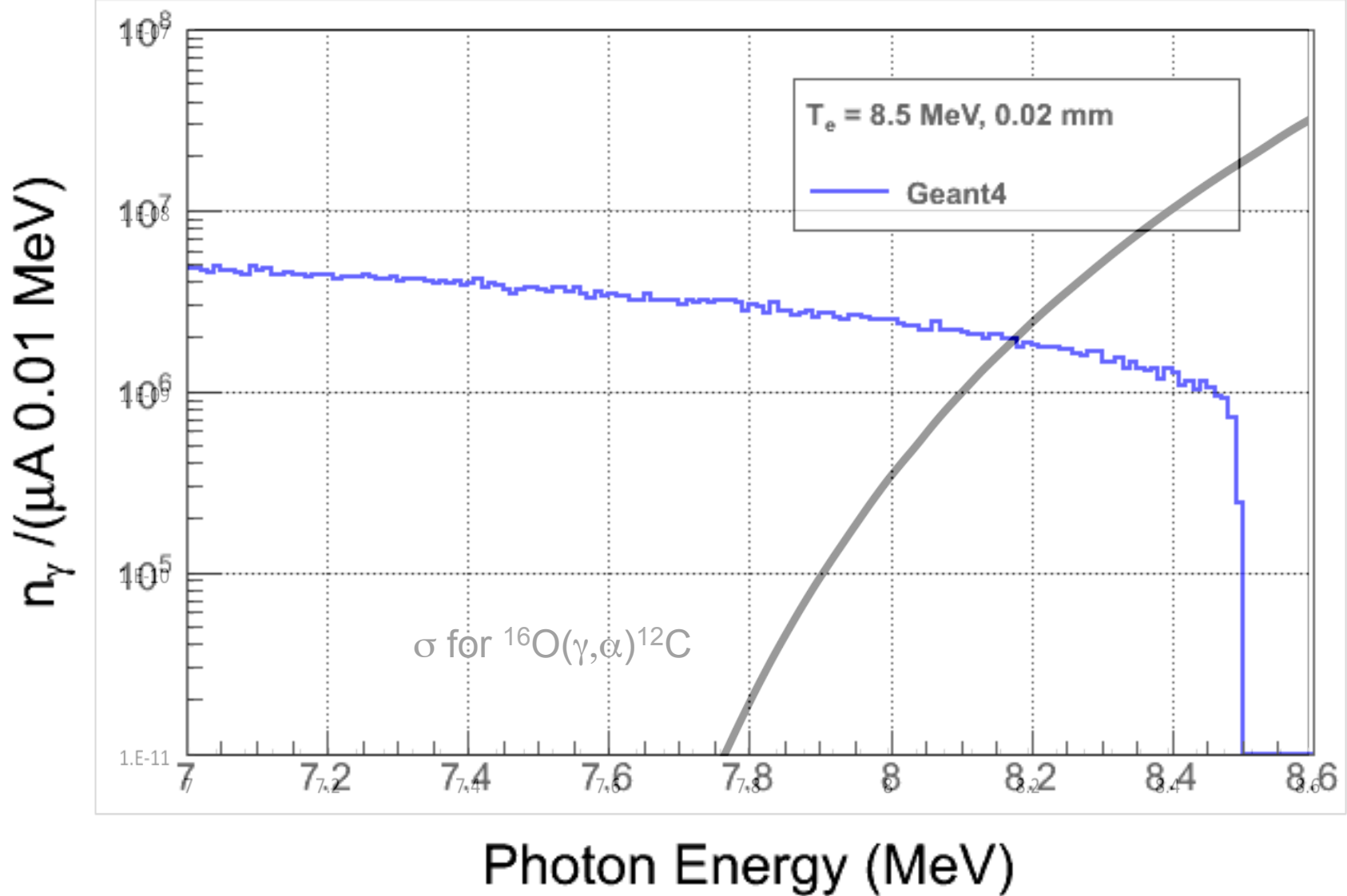
# Experimental setup



# Experimental Setup

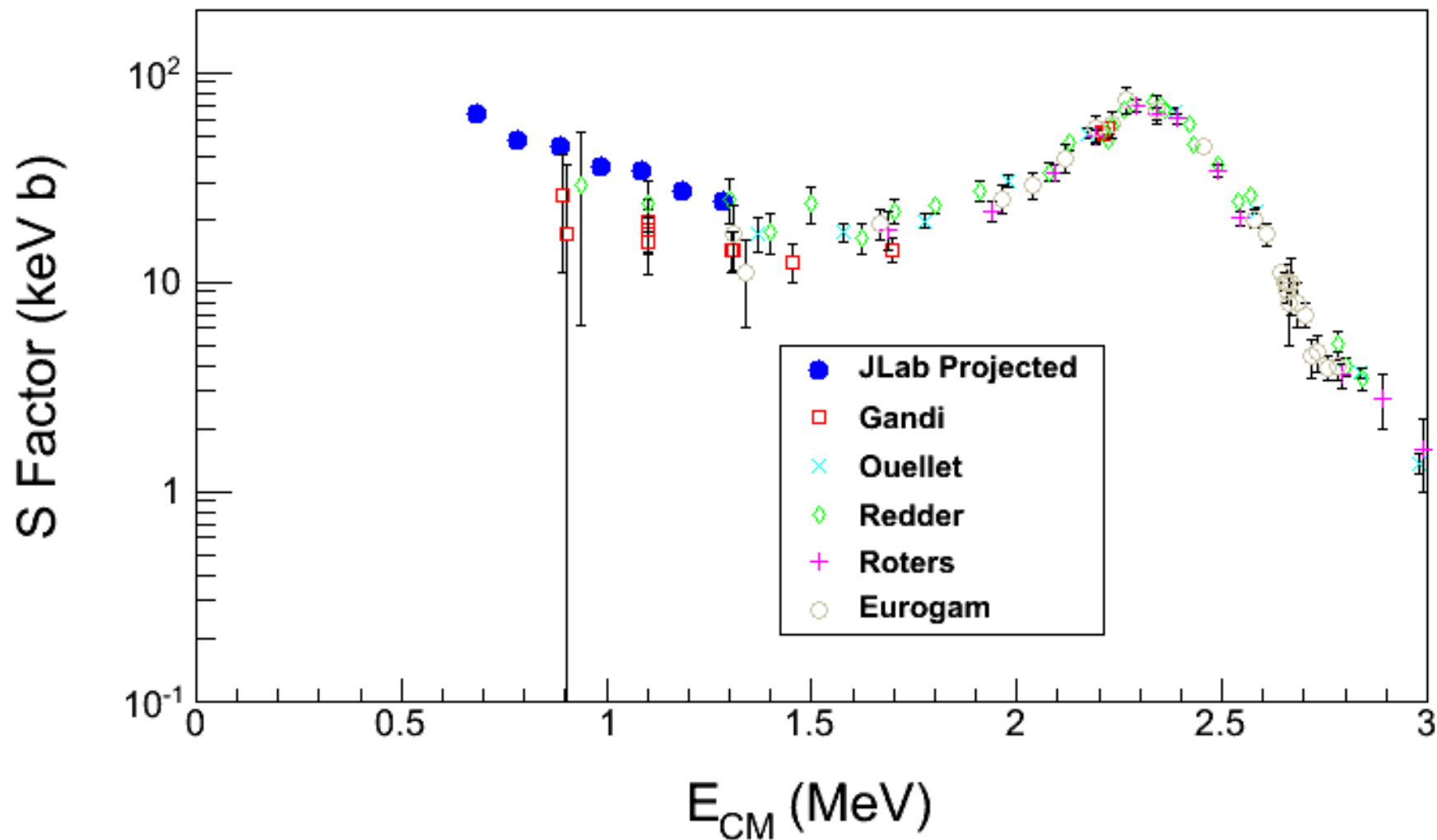








# Statistical error bars



# Systematics

Source	Systematic Error (%)
Absolute beam energy	11-28
Beam current	3
Photon flux	5
Radiator thickness	3
Target thickness	3
Bubble chamber efficiency	5

With improvement  $dE_e \sim 0.2\%$

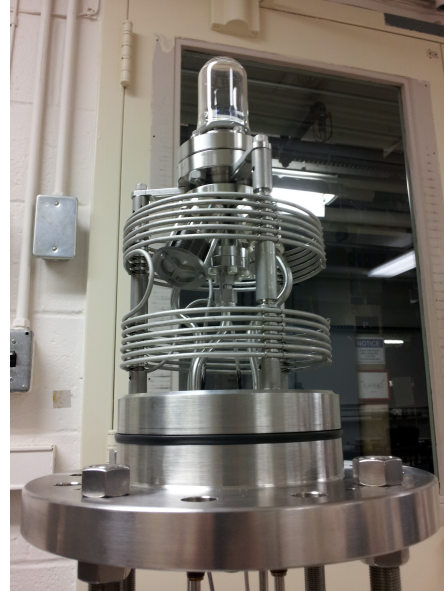
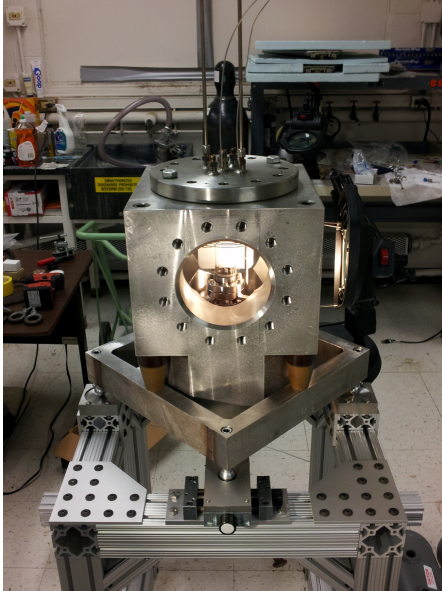
# Summary of beam time request (336 h)

- Commissioning (32 h)
  - Radiator and Dump : 8 h
  - Bubble chamber : 24 h
- Background measurements (120 h)
  - $^{18}\text{O}(\gamma,\alpha)^{14}\text{C}$ : 70 h (3 h per energy + 2h energy change) (14 energies)
  - $^{17}\text{O}(\gamma,\alpha)^{13}\text{C}$ : 50 h (3 h per energy + 2h energy change) (10 energies)
- $^{16}\text{O}(\gamma,\alpha)^{12}\text{C}$ : (184 h, includes 2 h energy change per energy)

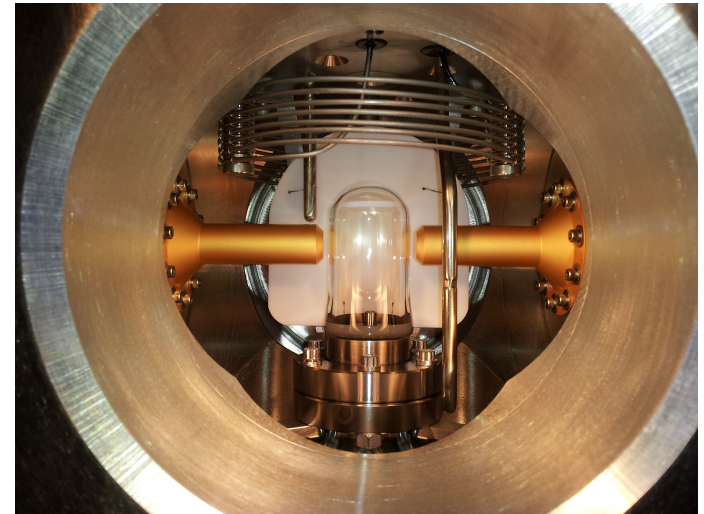
# Summary

- We plan to expose for the first time the bubble chamber to a bremsstrahlung beam
- We plan to obtain  $^{12}\text{C}(\alpha,\gamma)^{16}\text{O}$  cross sections
- Background information would be obtained for  $^{18}\text{O}(\gamma,\alpha)$ ,  $^{17}\text{O}(\gamma,\alpha)$

Our proposal requests 336 hours of injector beam time.  
These include time for commissioning and energy changes.



Oxygen STAR



# Penfold-Liess Unfolding

Bubble Chamber Collaboration

June 11, 2013

When using the continuous spectrum of Bremsstrahlung photon beam to study photo-nuclear reactions, the measured quantity is a yield. The yield (number of interactions) is a convolution of the cross section with the Bremsstrahlung spectrum:

$$y(E) = \int_{Threshold}^E N_{\gamma}(E, k)\sigma(k)dk, \quad (1)$$

where  $E$  is the electron beam kinetic energy,  $N_{\gamma}(E, k)$  is the number of gammas per energy unit which depends on the electron energy and the gamma energy. The continuous range of photon energies means that the cross section is not measured directly, instead it must be unfolded from the measured yields.

An integral equation of this form is known as Volterra Integral Equation of the First Kind. Mathematically the problem is one of numerical solution of the yield integral equation and  $\sigma(k)$  is the function to be solved for. One way to solve this equation is to use the Method of Quadratures (a method for constructing an approximate solution of an integral equation based on the replacement of integrals by finite sums). First the yields are measured at  $E = E_1, E_2, \dots, E_n$  where  $E_i - E_{i-1} = \Delta$ ,  $i = 2, \dots, n$ . Then,

$$y(E_i) = \int_{Threshold}^{E_i} N_{\gamma}(E_i, k)\sigma(k)dk \approx \sum_{j=1}^i N_{\gamma}(E_i, \Delta, k_j)\sigma(k_j), \quad (2)$$

where  $N_{\gamma}(E_i, \Delta, k_j)$  is the number of gammas in the energy bin of width  $\Delta$ .

Equation 2 is a set of linear equations which can be written in the matrix form:

$$\begin{pmatrix} y_1 \\ y_2 \\ \vdots \\ y_n \end{pmatrix} = \begin{pmatrix} N_{11} & 0 & \cdots & 0 \\ N_{21} & N_{22} & \cdots & 0 \\ \vdots & \vdots & \ddots & \vdots \\ N_{n1} & N_{n2} & \cdots & N_{nn} \end{pmatrix} \begin{pmatrix} \sigma_1 \\ \sigma_2 \\ \vdots \\ \sigma_n \end{pmatrix}. \quad (3)$$

This matrix equation can be solved with matrix inversion. Equivalently, the solution to Equation 2 can be written:

$$\sigma_i = \frac{1}{N_{ii}} \left[ y_i - \sum_{j=1}^{i-1} (N_{ij}\sigma_j) \right]. \quad (4)$$

The error propagation of Equation 4 is given by:

$$\left( \frac{d\sigma_i}{\sigma_i} \right)^2 = \frac{[(dy_i)^2 + \sum_{j=1}^{i-1} (N_{ij}d\sigma_j)^2]}{\left[ y_i - \sum_{j=1}^{i-1} (N_{ij}\sigma_j) \right]^2}. \quad (5)$$

For mono-chromatic photon beam, Equation 5 reduces to:

$$\left( \frac{d\sigma_i}{\sigma_i} \right)^2 = \left( \frac{dy_i}{y_i} \right)^2 = \frac{1}{y_i}. \quad (6)$$

Initially, the above unfolding method known as Penfold-Liess unfolding ([1]) (aka the Inverse-Matrix Method) gave unreliable results (see for example [2] and Figure 1) because (in the sixties and seventies) the unfolding procedures have been often considered in isolation from the photon energy spectrum of the bremsstrahlung beam used experimentally. At that time, experimentalists used the Schiff theoretical formula ([3]) to calculate  $N_{ij} = \Delta N_{\text{Schiff}}(E_i, k_j - \Delta/2)$ . Findlay proposed ([4]) that a simple modification to  $N_{ij}$  prevents the generation of spurious results. He replaced  $k - \Delta/2$  by  $k - \lambda\Delta$  where  $\lambda$  is a parameter determined by considering the energy spread of the electron beam and the energy loss of the electron beam in the radiator. Findlay's modification was successfully demonstrated to produce correct cross sections in ([5], see Figure 2, [6]).

These days, there are very accurate Monte-Carlo simulations,  $N_{ij}$  can be calculated for each specific experimental conditions without the need to use theoretical formula. This removes problems in the unfolding related to the knowledge of  $N_{ij}$ .

However, this is not the only reason that may cause Penfold-Liess unfolding to fail. Careful inspection of Equation 5 reveals that statistical errors

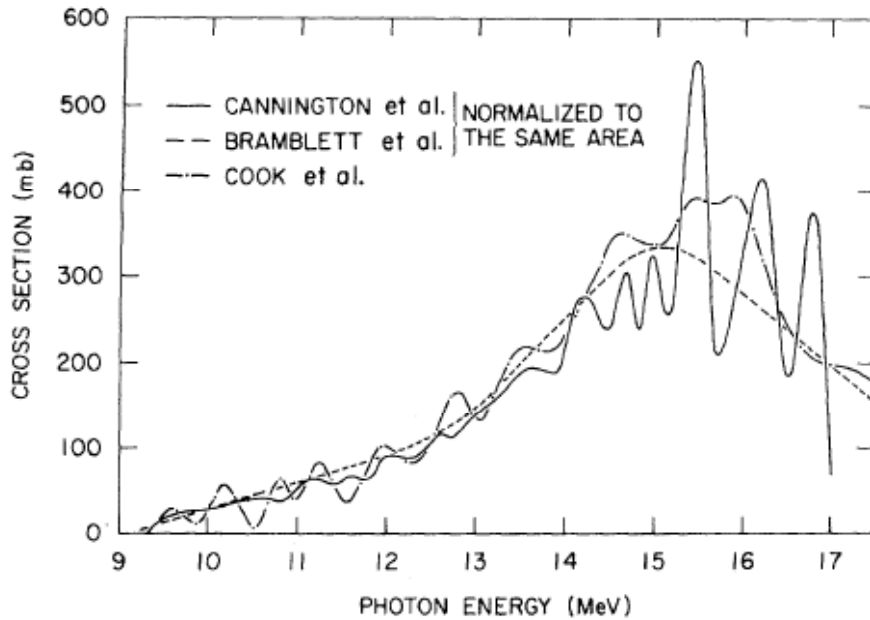


Figure 1: Comparison of the  $^{141}\text{Pr}(\gamma, n)$  cross sections. Cook and Cannington were done with Bremsstrahlung beams. The correct cross section by Bramblett (dashed line) was done with a monochromatic gamma beam from positron annihilation in flight.

of the measured yields play a role in two ways. First, the statistical errors add up as can be seen in the numerator of the right hand side of Equation 5. Although  $\sigma_1$  and probably  $\sigma_2$  will be very closed to their real values, the remaining cross section data points will start to oscillate. Second, the denominator of the difference of two large numbers and thus will enhance the error in the cross section since the difference will be a smaller number. Indeed, having a very steep cross section is an advantage here, since it reduces the second term in the denominator and give a denominator with large number. To determine the required statistical error for each yield measurement, the steepness of the cross section must be taken into account. A relatively flat cross section requires very accurate yield measurements to be able to successfully unfold the cross section.

Indeed, the  $^{16}\text{O}(\gamma, \alpha)^{12}\text{C}$  cross section is very steep (shown in Figure 3) and only photons near the endpoint contribute to the yield for each

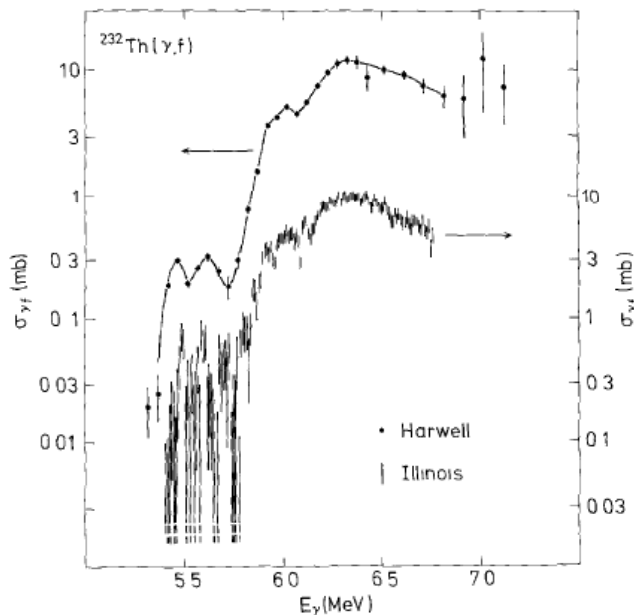


Figure 2: Photofission of  $^{232}\text{Th}$  near threshold. Solid circles present data from [5] with Bremsstrahlung beam and lines data with tagged photon beam.

beam energy, see Figure 4. Similar arguments show that it is beneficial to maximize the number of gammas near the endpoint relative to the number of gammas at lower gamma energies,  $N_{ii}/N_{ij}$ ,  $j = 1, \dots, i - 1$ . Figure 5 shows the Schiff Bremsstrahlung cross section for 8.5 MeV electron beam kinetic energy. This is one reason, among many others, why we choose to run with a very thin Bremsstrahlung radiator. Figure 6 shows the Bremsstrahlung yield for three different radiator thicknesses.

As was discussed above, poor statistics will cause the unfolded cross section to oscillate as a function of photon energy especially at energies above the giant resonance energy where the cross section is flat or decreasing. These cross sections are unacceptable physically and smoothing must be used. Under the assumption of the cross section smoothness, the deconvolution method is known as the Regularization Method. There are several kinds of regularization methods such as Cook's Least Structure Method [7], the Second Difference Method [8] and Tikhonov Regularization [9].

Another deconvolution method is called the Photon Difference Method [10]. In this method a nearly mono-energetic photon spectrum can be constructed artificially by taking an algebraic sum of three Bremsstrahlung



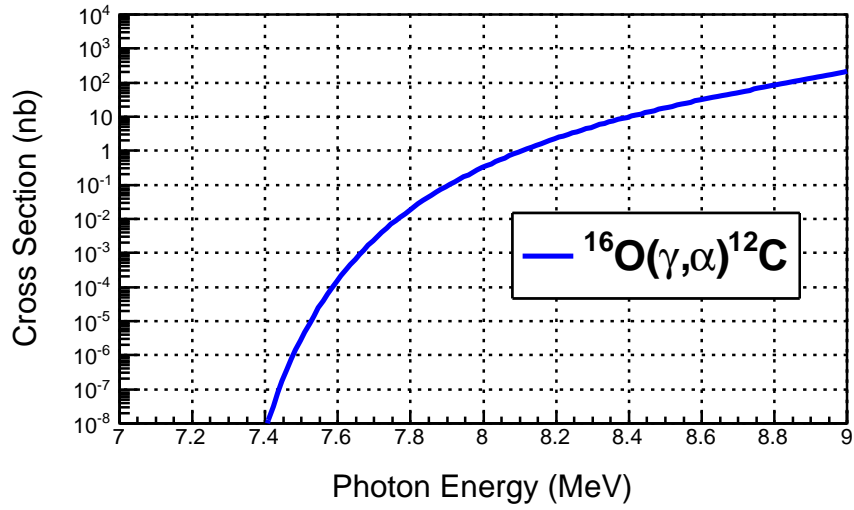


Figure 3: The cross section of  $^{16}\text{O}(\gamma, \alpha)^{12}\text{C}$ .

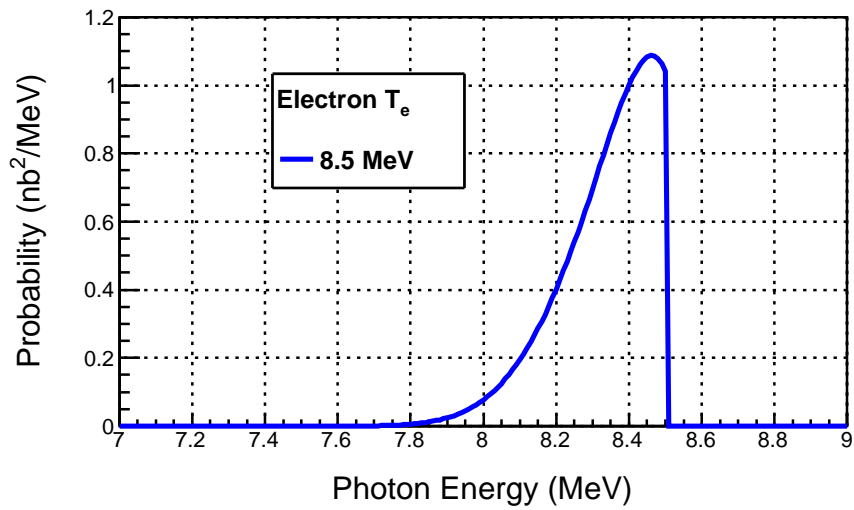


Figure 4: The probability of Bremsstrahlung photons to undergo the interaction  $^{16}\text{O}(\gamma, \alpha)^{12}\text{C}$ .

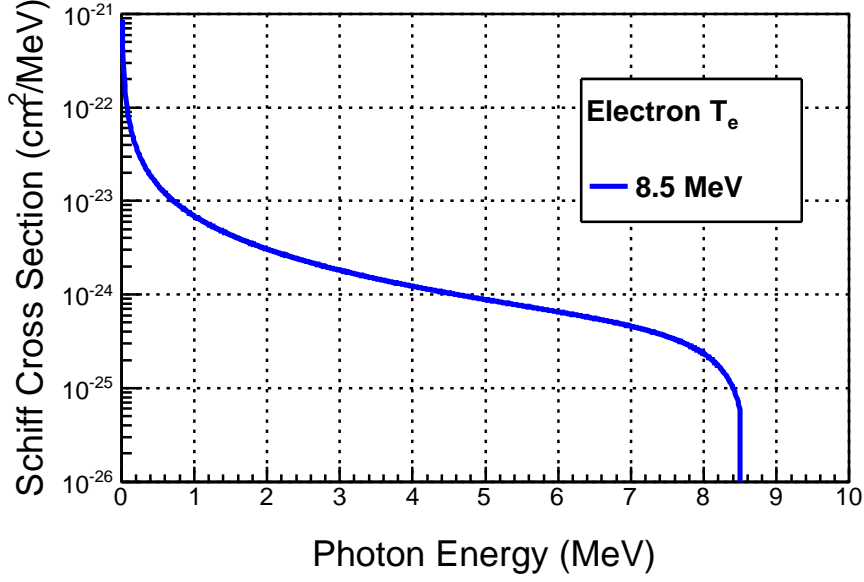


Figure 5: Schiff Bremsstrahlung cross section for a Cu radiator.

spectra with consecutive endpoint energies:

$$\phi_M(E_i) = \phi_{\text{Schiff}}(E_i) - a \phi_{\text{Schiff}}(E_{i-1}) + b \phi_{\text{Schiff}}(E_{i-2}), \quad (7)$$

where  $\phi_{\text{Schiff}}(E_i)$  is the Schiff Bremsstrahlung spectrum with endpoint energy  $E_i$  and the parameters  $a$  and  $b$  are both positive and chosen such that  $\phi_M(E_i)$  represent a mono-energetic photon spectrum. An example is shown in Figure 7 where:

$$\phi_M(8.5) = \phi_{\text{Schiff}}(8.5) - 1.35 \phi_{\text{Schiff}}(8.4) + 0.30 \phi_{\text{Schiff}}(8.3). \quad (8)$$

A differential yield spectrum can be constructed artificially by using the same linear combination of the corresponding yields. Then, the photo-nuclear cross section is simply the ratio of this differential yield to the corresponding mono-energetic photon flux.

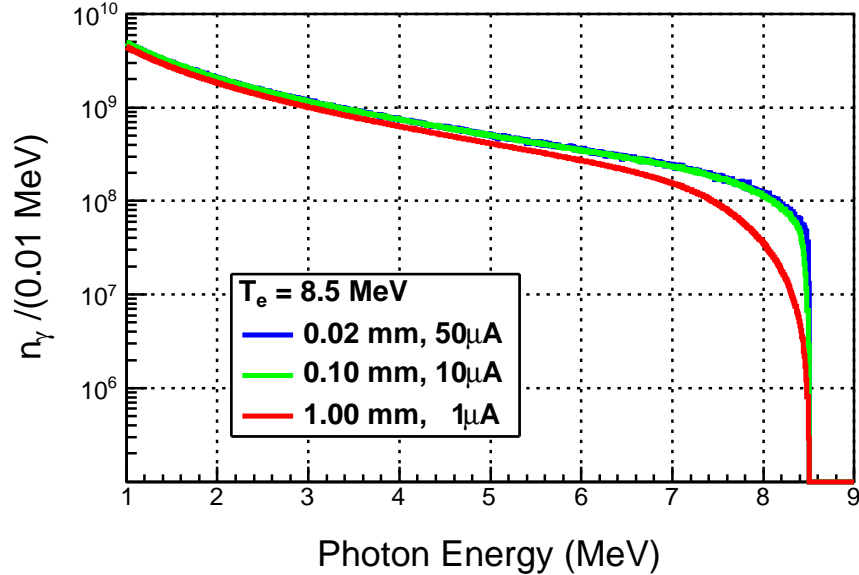


Figure 6: Bremsstrahlung yield for three different radiator thicknesses.

## References

- [1] A. S. Penfold and J. E. Leiss, Analysis of photonuclear cross sections. *Phys. Rev.* **114**, 1332 (1959).
- [2] R. E. Sund *et al.*,  $^{141}\text{Pr}(\gamma, n)$  Cross Section from Threshold to 24 MeV. *Phys. Rev. C* **2**, 1129 (1970).
- [3] L. I. Schiff, Energy-Angle Distribution of Thin Target Bremsstrahlung. *Phys. Rev.* **83**, 252 (1951).
- [4] D. J. S. Findlay, A Modification to the Penfold-Leiss Method of Cross Section Unfolding. *Nucl. Inst. Meth.* **213**, 353 (1983).
- [5] D. J. S. Findlay *et al.*, Photofission of  $^{232}\text{Th}$  near threshold. *Nucl. Phys. A* **458**, 217 (1986).
- [6] S. J. Watson *et al.*, Photofission and photoneutron measurements on  $^{241}\text{Am}$  between 5 and 10 MeV. *Nucl. Phys. A* **548**, 365 (1992).

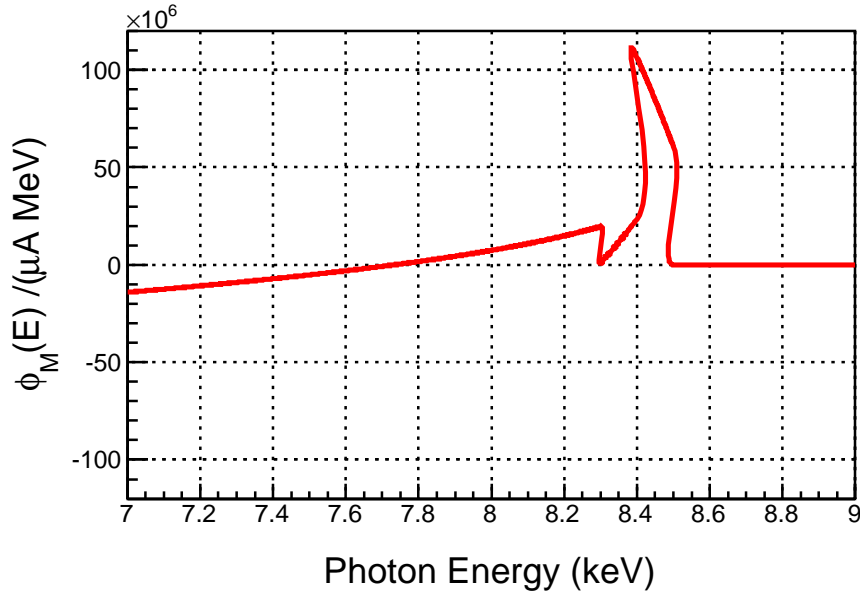


Figure 7: Mono-energetic photon spectrum constructed artificially by taking an algebraic sum of three Bremsstrahlung spectra with consecutive endpoint energies.

- [7] B. C. Cook, Least Structure Solution of Photonuclear Yield Functions. Nucl. Inst. Meth. **24**, 256 (1963).
- [8] K. N. Geller and E. G. Muirhead, High Resolution Second difference Analysis of Photonuclear Yield Curves. Nucl. Inst. Meth. **26**, 274 (1964).
- [9] A. N. Tikhonov *et al.*, About the determination of photonuclear reaction cross-sections. Vestn. Mosk. Univ., Ser. III. Fiz. Astron. 11: No. **2**, 208 (1970).
- [10] E. Van Camp *et al.*, Experimental determination of the proton escape width in the giant dipole resonance  $^{89}\text{Y}$ . Phys. Rev. C **24**, 2499 (1981).